Formation of Contact Ion Pairs and Solvation of Li+ Ion in Sulfones: Phase Diagrams, Conductivity, Raman Spectra, and Dynamics†

ARTICLE *in* JOURNAL OF CHEMICAL & ENGINEERING DATA · FEBRUARY 2010

Impact Factor: 2.04 · DOI: 10.1021/je9009249

5 AUTHORS, INCLUDING:

Kamil Rabadanov
Russian Academy of Sciences
17 PUBLICATIONS **29** CITATIONS
SEE PROFILE

Sviatoslav Kirillov
Joint Department of Electrochemical Ener…
91 PUBLICATIONS **537** CITATIONS
SEE PROFILE

Formation of Contact Ion Pairs and Solvation of Li^+ Ion in Sulfones: Phase Diagrams, Conductivity, Raman Spectra, and Dynamics†

Dmytro O. Tretyakov,‡ Vitaly D. Prisiazhnyi,‡ Malik M. Gafurov,§ Kamil Sh. Rabadanov,§ and Sviatoslav A. Kirillov*,‡,||

Joint Department of Electrochemical Energy Systems, 38A Vernadsky Ave., 03142 Kyiv, Ukraine, Kh. A. Amirkhanov Institute of Physics and Analytical Center of Common Access, 94 M. Yaragsky St., 367003, Russian Federation, and Institute for Sorption and Problems of Endoecology, 13 Gen. Naumov St., 03164 Kyiv, Ukraine

This work reports phase diagrams, conductivity isotherms, and data regarding the structure and dynamics of systems formed by lithium perchlorate and nitrate as solutes and sulfones as solvents. The $LiClO_4 + (CH_3)_2SO_2$ system behaves like typical electrolytic systems containing a lithium salt and a solvent and forms a 1:1 solvate; its conductivity isotherm demonstrates a maximum. Unlike typical systems, the phase diagrams of the $LiNO_3 + (CH_3)_2SO_2$ and $LiNO_3 + (C_2H_5)_2SO_2$ systems appear to be simple eutectic. The dependences of specific conductivity on the concentration of $LiNO_3$ are also uncommon showing no maximum characteristic to electrolyte solutions. Raman studies and analysis of dynamics performed using Raman data signify that, in the $LiClO_4 + (CH_3)_2SO_2$ system, solvated cations and contact ion pairs exist. In the $LiNO_3 + (CH_3)_2SO_2$ system, contact ion pairs are present as well, but signatures of cation solvation cannot be found.

Introduction

One of the most valuable applications of solutions of lithium salts in dipolar aprotic solvents is their use in lithium ion batteries as electrolytes, that is, media ensuring the transfer of charges between two electrodes.[1,2] Ionic solutions as a whole and nonaqueous electrolytes for industrial applications in particular are subjects of continuous interest of chemists since the discovery of electrolytic dissociation. To consider if a lithium salt−solvent system meets the criteria of the battery practice, data regarding its phase diagram and conductivity are of primary importance, since the former determines the range of the liquid state of the system and the latter contributes to the ohmic losses of the battery which must be as small as possible. As a rule, phase diagrams of binary salt−solvent systems are of the distectic or peritectic type, revealing the presence of stable solvates, that is, compounds formed by the solute and solvent.[3,4] Concentration dependences of conductivity of these systems demonstrate a maximum,[3−6] reflecting interplay among various types of particles dominating in the solution, which may contain solvated cations and anions at low concentrations and several types of ion pairs and more complex aggregates (triplets, quadruplets, etc.) at higher concentrations of the solute. According to conductivity theories,[5,6] an increase in conductivity at low concentrations of the solute, when ion pairing is insufficient, can be associated with the growing number of charge carriers, whereas the maximum and further decrease of conductivity at high concentrations appear when ion pairing becomes pronounced and then prevails.

Understanding speciation in aqueous and nonaqueous electrolytes attracts much attention of experimentalists,[7−15] and vibrational spectroscopy is one of the most powerful tools in solving this valuable problem, enabling one to uncover the structure of entities present in solutions.[13−21] In particular, vibrational lines corresponding to "free" and ion-paired anions, as well as to solvent molecules located within and outside the solvation sphere of cations, are well-documented.[13] It should be mentioned, however, that from the point of view of dynamics, solutions of lithium salts in dipolar aprotic solvents are considered to contain short-lived solvates and ion pairs. According to simulation studies and relaxation measurements, residence times of solvent molecules in solvate spheres lie within the picosecond time domain,[10,14] thereby revealing just certain orientational ordering around cations. Residence times of cations and anions in ion pairs are also short and exceed the duration of life of solvation shells by an order of magnitude.[11]

Among electrolytes for battery applications, solutions of lithium salts in sulfones are especially interesting because of their high resistivity to electrode materials and ability to ensure high speed of electrode processes.[22] Furthermore, the properties of sulfones as solvents are unique because of their strikingly large dielectric constants (47.39 for dimethyl sulfone) and dipole moments (4.44 D for dimethyl sulfone) which, from the point of view of quantum chemistry, arise from an unexpectedly inhomogeneous distribution of the electrostatic potential on the surface of their molecules.[23] Although dimethyl sulfone has been introduced in electrochemical practice in 1994,[24] not so much work has been done in the field of phase diagrams, conductivity, and structure of sulfone-based electrolytes.[25−27] Another possible application of sulfone-containing systems is their use as the so-called salt−solvate electrolytes, namely, those formed by a mixture of a solvate and a salt (unlike a mixture of a solvate and a solvent as usual). It has been found that such electrolytes are advantageous owing to easing reduction processes in batteries with sulfur anodes[28] and ensuring high specific power of $Li-CF_x$ batteries.[29] Therefore, our aim in this paper was to study phase diagrams, to determine the conductivity, and to

† Part of the "Josef M. G. Barthel Festschrift".

* Corresponding author. Tel.: +380 44 424 35 72. Fax: +380 44 424 62 40. E-mail address: kir@i.kiev.ua.
‡ Joint Department of Electrochemical Energy Systems.
§ Kh. A. Amirkhanov Institute of Physics and Analytical Center of Common Access.
|| Institute for Sorption and Problems of Endoecology.

10.1021/je9009249
Published on Web 02/16/2010

characterize main structural entities in the systems formed by dimethyl and diethyl sulfone, on the one hand, and lithium nitrate and perchlorate, on the other.

It is a great pleasure to contribute to the Festschrift issue of the *Journal of Chemical and Engineering Data* in honor of Professor Joseph M. G. Barthel, because—due to his outstanding input in the theory and practice of ionic solutions summarized in numerous books, reviews, and regular articles, some of which[1,5,14] are referred to here—these topics and his name are inseparable.

Experimental Section

Sample Preparation. Lithium nitrate (Fluka, 99.0 %) and perchlorate (pure, Novosibirsk, Russia) were twice recrystallized from doubly distilled water and slowly dehydrated in vacuum until anhydrous salts were formed. These were dried in vacuum at 150 °C during at least 24 h. Dimethyl sulfone $(CH_3)_2SO_2$ and diethyl sulfone $(C_2H_5)_2SO_2$, both from Aldrich, ≥ 98 %, were twice recrystallized from doubly distilled water and sublimated in vacuum at (90 and 70) °C, respectively. The completeness of the water removal was checked by the melting points of the substances. All further operations with lithium salts and sulfones were performed in a dry glovebox. Remaining humidity in the glovebox was controlled with a digital hygrometer.

Phase Diagrams. Phase equilibria were studied by means of differential thermal analysis on a homemade computer-driven device using samples of the mass of ≈2.5 g. To homogenize the samples, these were premelted, kept in the molten state for approximately 0.2 h, cooled, and stored at ambient temperatures. Heating curves were registered after cooling the samples in a cooling block kept at $t \approx -100$ °C and equilibrating them for at least 1 h. Thermal analysis data for the systems studied, as well as representative thermal analysis curves, are given as Supporting Information.

Conductivity Measurements. Electrical conductivity was measured on a digital AC E7-14 immittance meter (Caliber, Minsk, Belarus) at the frequency of 10 kHz with a 0.5 % accuracy. A conductometric cell with planar platinum electrodes was used. Experimental values of conductivity κ were calculated according to the relation

$$\kappa = k/R \tag{1}$$

where k is the cell constant and R is the resistance of a solution. The cell constant was determined in measurements of conductivity of a 0.1 M aqueous solution of KCl at (0 to 32) °C and molten lithium nitrate at (240 to 280) °C. Temperature measurements were performed with the resolution of 0.05 K by means of a chromel−alumel thermocouple in conjunction with a voltage comparator. Temperature stability was better than 0.1 K. Tables of specific conductivity data for all systems studied are given as Supporting Information.

Spectroscopic Measurements. Stokes-side Raman spectra excited by means of an Ar ion laser (LG-106M, Plasma, Ryazan, Russia, $\lambda = 488$ nm, an output power of (300 to 600) mW) were recorded on a double monochromator (DFS-24, LOMO, St. Petersburg, Russia) in the 90° geometry. If a right-angle Raman scattering experiment is performed in two different polarization geometries, and the direction of the electric field of the incident radiation is vertical (V), scattered intensity of two kinds can be registered, namely, I_{VV} and I_{VH}. In I_{VV} the electric field of the scattered light propagates in the same direction as in the incident radiation (V), and in I_{VH} it is horizontal (H). Both I_{VV} and I_{VH} spectra were registered, and the so-called isotropic spectra were calculated as

$$I_{iso}(\nu) = I_{VV}(\nu) - \frac{4}{3} I_{VH}(\nu) \tag{2}$$

where ν is the frequency measured in wavenumbers (cm^{-1}), with an uncertainty in $I_{iso}(\nu)$ of less than 3 %. The instrumental resolution was fixed at 0.2 cm^{-1} for the whole set of measurements, and the temperature was controlled with an uncertainty of 1 K. Samples were flame-sealed in Pyrex tubes with an inner diameter of 5 mm.

Results and Discussion

Phase Diagrams. The phase diagram of the $LiClO_4 + (CH_3)_2SO_2$ system is presented in Figure 1, top panel. The formation of a 1:1 solvate, which melts congruently at 127 °C, is evident. Mixtures of this solvate with the solvent and the salt form eutectics containing (31.0 and 60.0) % mole fraction of $LiClO_4$ and have melting temperatures of (49 and 108) °C, respectively. The thermal data for other possible solvates (1:4, 20 % mole fraction of $LiClO_4$; 1:2, 33 % mole fraction of $LiClO_4$; 2:1, 66 % mole fraction of $LiClO_4$) are difficult to interpret because the differential thermal analysis peaks severely overlap. An attempt to use X-ray diffraction to distinguish the phases present was unsuccessful, so that the exact nature of thermal effects, especially those denoted in Figure 1, top panel, by empty circles remains unknown.

The phase diagrams of the $LiNO_3 + (CH_3)_2SO_2$ and $LiNO_3 + (C_2H_5)_2SO_2$ systems are shown in Figures 2 and 3, top panels; respective data files can be found in the Supporting Information. Unexpectedly, they demonstrate a single eutectic shape with eutectic points at (30.0 and 15.0) % mole fraction of $LiNO_3$ and melting temperatures of (77 and 65) °C, respectively. Such a shape of phase diagrams is abnormal to systems containing lithium salts and dipolar aprotic solvents, evidencing no specific interaction between the components of the system. As mentioned above, typical phase diagrams of binary salt−solvent systems are those of distectic or peritectic type, reflecting the presence of compounds formed by the solute and solvent (solvates).[3,4,30]

Some conclusions regarding interactions in a system can be drawn from the analysis of phase diagrams. As follows from thermodynamics, in the region close to the neat solvent in an ideal binary solution containing a hypothetical, undissociated solute, where the enthalpy of mixing is of zero value and the process of dissolution is entropy-driven, the mole fraction x_i of the solute i is expressed as[31]

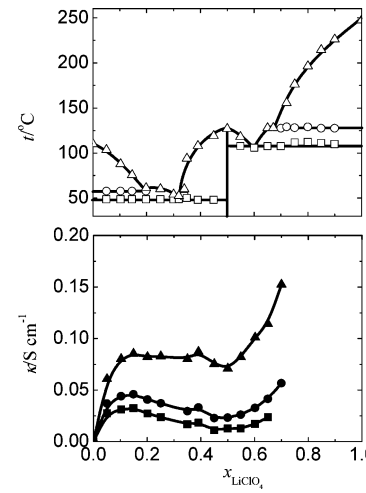

Figure 1. Phase diagram (top panel) and specific conductivity isotherms (bottom panel) for the $LiClO_4 + (CH_3)_2SO_2$ system. ■, 125 °C; ●, 150 °C; ▲, 200 °C.

$$\ln x_i = -\frac{\Delta H_{m,i}}{R}\left(\frac{1}{T} - \frac{1}{T^*}\right) \quad (3)$$

where $\Delta H_{m,i}$ is the enthalpy of melting of the pure component i at the melting point T^* [K], R is the gas constant, and T is the temperature of the liquidus [K]. Equation 3 is widely used for calculations of liquidus curves and studies of dissociation in melts; see ref 32 as an example. Thermodynamic data required for calculations of the liquidus curves using eq 3 taken from ref 33 are $\Delta H_{m,LiClO_4} = (16.987 \pm 0.041)$ kJ·mol^{-1}, $\Delta H_{m,LiNO_3} = (25.522 \pm 0.418)$ kJ·mol^{-1}, $\Delta H_{m,(CH_3)_2SO_2} = (20.501 \pm 0.836)$ kJ·mol^{-1}, and $\Delta H_{m,(C_2H_5)_2SO_2} = (18.409 \pm 2.092)$ kJ·mol^{-1}. The results of such calculations (Figure 4) signify that the $LiClO_4 + (CH_3)_2SO_2$ system is far from ideality and does not obey eq 3, whereas both nitrate-containing systems follow eq 3 much better. A noncoincidence between the experimental points and the calculated curve for the diethyl sulfone-rich part of the $LiNO_3 + (C_2H_5)_2SO_2$ system may be caused by uncertainties in the value of $\Delta H_{m,(C_2H_5)_2SO_2}$.

Conductivity Isotherms. Typical specific conductivity isotherms for electrolyte solutions reflect interactions between the solute and the solvent and display a maximum.[3−6] An ascending part of the isotherm reflects an increase in the number of charge carriers, and a descending part arises from ion pairing and the growth of viscosity.[5,6] This is true for the $LiClO_4 + (CH_3)_2SO_2$ system where the presence of a maximum at low concentrations of the salt is obvious (Figure 1, bottom panel, see also a data file in Supporting Information). As far as the second maximum at ~40.0 % molar fraction of $LiClO_4$ is concerned, its presence verified with at least three different samples may be due to the dissociation of the solvate formed at low concentrations. Similar behavior has been already noticed in the $LiBF_4 + (CH_3)_2SO_2$ system.[27] It should be mentioned that second maxima on conductivity isotherms have also been found for solutions of $LiClO_4$ and $LiN(SO_2CF_3)_2$ in boron acid esters of glycol,[34] but no explanation of this intriguing fact has been given.

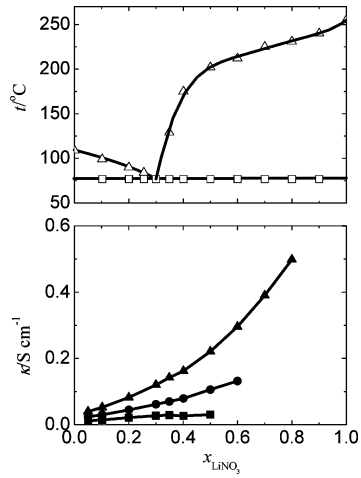

Figure 2. Phase diagram (top panel) and specific conductivity isotherms (bottom panel) for the $LiNO_3 + (CH_3)_2SO_2$ system. ■, 150 °C; ●, 200 °C; ▲, 250 °C.

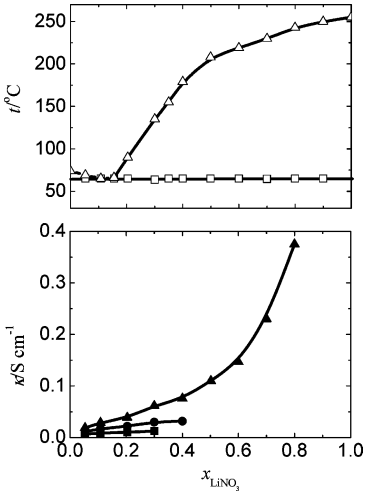

Figure 3. Phase diagram (top panel) and specific conductivity isotherms (bottom panel) for the $LiNO_3 + (C_2H_5)_2SO_2$ system. ■, 150 °C; ●, 200 °C; ▲, 250 °C.

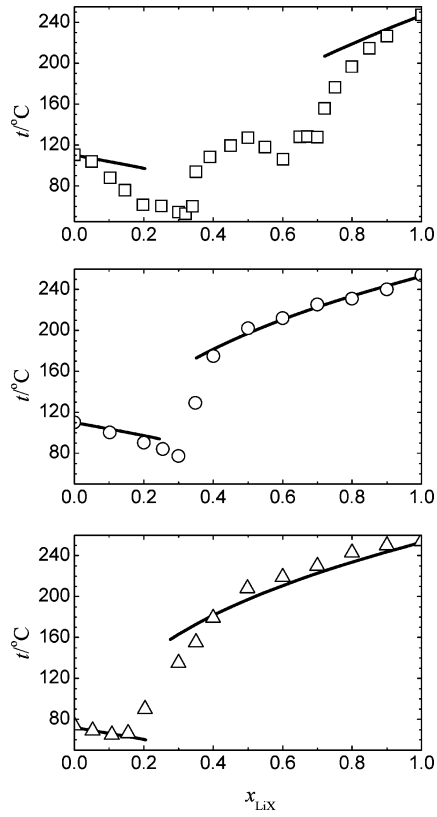

Figure 4. Experimental data (points) and calculated liquidus curves (lines) for the systems studied. □, $LiClO_4 + (CH_3)_2SO_2$; ○, $LiNO_3 + (CH_3)_2SO_2$; △, $LiNO_3 + (C_2H_5)_2SO_2$.

In Figures 2 and 3, bottom panels, isotherms of the specific conductivity are shown for the $LiNO_3 + (CH_3)_2SO_2$ and $LiNO_3 + (C_2H_5)_2SO_2$ systems; respective data files can be found in the Supporting Information. Unlike isotherms for other electrolytes, these demonstrate a smooth increase in conductivity to the values characteristic of molten $LiNO_3$. One can conclude that either the maximum of conductivity is absent in these systems or it is insignificant and lies at concentrations close to the neat sulfone. Anyway, the absence of a distinct conductivity maximum may signify that both dissociation and solvation processes are suppressed in the systems studied.

Spectroscopic Data: Line Frequencies. To understand these unexpected data, Raman spectroscopy has been employed to the $LiClO_4 + (CH_3)_2SO_2$ and $LiNO_3 + (CH_3)_2SO_2$ systems. In both cases, solutions containing 30.0 % mole fraction of lithium salts have been used. For such high concentrations of lithium salts, the presence of free and/or solvated ions and contact ion pairs can be expected, whereas the formation of solvent-shared and/or solvent-separated ion pairs seems impossible because of the lack of solvent (1 Li^+ per 2.33 molecule of sulfone). Overall

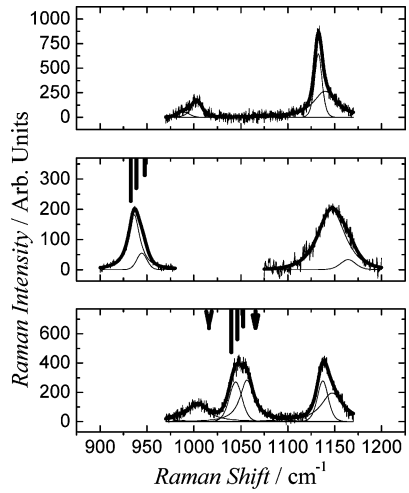

Figure 5. Raman spectra of dimethyl sulfone (top panel) and its solutions containing 30 % mole fraction of $LiClO_4$ (middle panel) and $LiNO_3$ (bottom panel) at 180 °C. Thick lines are the measured spectra. Thin lines represent a decomposition of these spectra according to the method described in refs 35 to 37. Long, medium, and short bars in the middle and bottom panels indicate the positions of Raman lines corresponding to free anions, anions in solvent-separated ion pairs, and anions in contact ion pairs, respectively. An empty arrow in the bottom panel stands for the position of the Raman line corresponding to the nitrate ion in the matrix isolated $Li^+ NO_3^-$ contact ion pair, and a filled arrow indicates the position of the Raman line corresponding to the nitrate ion in molten $LiNO_3$.

spectra presented in Figure 5 have been decomposed according to the method described in refs 35 to 37.

A region between (850 and 1250) cm^{-1} has been studied. It contains the most intense lines of both inorganic ions and dimethyl sulfone. Specifically, in this region, the lines corresponding to the totally symmetric vibrations of perchlorate and nitrate ion, namely, $\nu_1(A_1)$ of ClO_4^- and $\nu_1(A'_1)$ of NO_3^-, are showing up at ≈940 cm^{-1} and ≈1050 cm^{-1}, respectively,[38] and two strong lines of dimethyl sulfone are observed at (1130 and 1000) cm^{-1}.[39] The former, denoted as $\nu_5(A_1)$, corresponds to the symmetrical stretching of the SO_2 group, which is most sensitive to the coordination of sulfone by cations.[26,40] The latter, denoted as $\nu_6(A_1)$, corresponds to the bending vibrations of the CH_3 group. Weak lines of $(CH_3)_2SO_2$ in this region are $\nu_{25}(B_2)$ at 990 cm^{-1} and $\nu_7 + \nu_8(A_1)$ at (1140 to 1145) cm^{-1}.[39] In this paper, we confine ourselves to the most characteristic features of Raman spectra, namely, the lines of anions and the strongest $\nu_5(A_1)$ line of dimethyl sulfone.

As follows from spectroscopic studies of solvation and ion pairing, in diluted solutions,[13,16] the line belonging to unperturbed, free ClO_4^- is showing up at (932 to 934) cm^{-1}. Upon rising concentration, this line undergoes negligible shift and becomes asymmetric due to some extra lines emerging on its high-wavenumber side. The line at (938 to 939) cm^{-1} belongs to solvent-separated ion pairs[13,16] where perturbations of the anion are quite significant, and the line at (944 to 946) cm^{-1} reflects the presence of contact ion pairs[13,16] where perturbations of the anion are the strongest. The sequence for solutions of $LiNO_3$ is similar:[13,41] ≈1042 cm^{-1} for unperturbed, free NO_3^- ions; (1044 to 1047) cm^{-1} for solvent-separated ion pairs; ≈1052 cm^{-1} for ion aggregates (triplets or contact ion pairs). It is noticeable that, in different solvents, such sequences are the same.[13]

In the case of solvents molecules, their perturbations arising from interactions with cations are even stronger. The vibrational lines corresponding to unperturbed, free molecules and to molecules surrounding cations can often be observed separately.[13] This means that signatures of solvation of cations in solutions are easier to discern, if compared with those of ion pairing.

Table 1. Peak Positions ν, Dephasing Times τ_V, Second Moments $M(2)$, and Modulation Times τ_ω for Vibrations of Dimethyl Sulfone Molecules and Perchlorate and Nitrate Ions, in Raman Spectra of Dimethyl Sulfone and 30 % Solutions of Lithium Perchlorate and Nitrate in It, and in Molten Lithium Nitrate

liquid or solution	assignment	ν/cm^{-1}	t/°C	τ_V/ps	$M(2)$/ps^{-2}	τ_ω/ps
	Dimethyl Sulfone Molecules					
$(CH_3)_2SO_2$	$\nu_5(A_1)$, SO_2 group	1132	180	1.53	0.77	2.82
$(CH_3)_2SO_2 + LiClO_4$	$\nu_5(A_1)$, SO_2 group	1145	200	0.46	13.5	0.29
$(CH_3)_2SO_2 + LiNO_3$	$\nu_5(A_1)$, SO_2 group	1137	180	1.32	1.04	5.06
	Perchlorate Ions					
$(CH_3)_2SO_2 + LiClO_4$	$\nu_1(A_1)$, free ClO_4^-	936	200	0.71	18.7	0.085
$(CH_3)_2SO_2 + LiClO_4$	ion pair	942	200	1.22	1.23	3.51
	Nitrate Ions					
$(CH_3)_2SO_2 + LiNO_3$	ion pair	1044	180	0.93	2.16	2.33
$(CH_3)_2SO_2 + LiNO_3$	$\nu_1(A'_1)$, free NO_3^-	1056	180	0.67	17.7	0.076
molten $LiNO_3$[51,52]	$\nu_1(A'_1)$, free NO_3^-	1067	255	0.49	15.0	0.17

On the basis of this information and the peak frequencies found in decomposition procedures (Figure 5, Table 1), the following differences in the molecular structure of the $LiClO_4 + (CH_3)_2SO_2$ and $LiNO_3 + (CH_3)_2SO_2$ systems can be noticed. Solvation of Li^+ seems evident in the $LiClO_4 + (CH_3)_2SO_2$ system, where the $\nu_5(A_1)$ line of $(CH_3)_2SO_2$ is blue-shifted (and broadened) significantly if compared to the neat dimethyl sulfone, and the intensity of the $\nu_7 + \nu_8(A_1)$ line becomes negligibly small. On the other hand, the profiles of the $\nu_5(A_1)$ and $\nu_7 + \nu_8(A_1)$ lines in the neat dimethyl sulfone and the $LiNO_3 + (CH_3)_2SO_2$ system undergo minor changes and probably indicate no cation solvation.

The lines corresponding to the ν_1 vibrations of perchlorate and nitrate anions are distinctly asymmetric. According to the positions of split lines obtained in decomposition procedures, free anions and contact ion pairs seem to be present in both systems.

A more detailed description of the molecular structure of the systems under investigation can be obtained in the study of dynamics based on spectroscopic data.

Spectroscopic Studies of Dynamics. The nature of entities existing in solutions can be understood in terms of theories of relaxation phenomena.[42,43] It has long been known that perturbations of a particle in a liquid by its nearest neighbors occurring with a characteristic time τ_ω modulate the vibrational frequency and cause vibrational phase shifts. Such a phenomenon is called vibrational dephasing and can be studied by means of an analysis of isotropic line profiles.[44] In brief, the isotropic line profile $I(\nu)$ corresponds to the so-called time-correlation function of vibrational dephasing $G_V(t)$, and $G_V(t)$ and $I_{iso}(\nu)$ are interrelated by the Fourier transform,

$$G_V(t) = \int_{-\infty}^{+\infty} I_{iso}(\nu) \exp(2\pi i c \nu t) d\nu \qquad (4)$$

where c is the speed of the light and t is the time. Computing time-correlation functions of vibrational dephasing according to eq 4 and integrating them, one finds the dephasing time τ_V, which reflects the speed of dephasing processes caused by interactions in a liquid. Furthermore, dephasing processes can be modeled in terms of the Kubo model,[45]

$$G_V(t) = \exp\{-M(2)\tau_\omega^2[\exp(-t/\tau_\omega) - 1 + t/\tau_\omega]\} \qquad (5)$$

where τ_ω is the modulation time and

$$M(2) = \int_{-\infty}^{\infty} \nu^2 I_{iso}(\nu)\, d\nu \quad (6)$$

is the second spectral moment of the Raman line (perturbation dispersion). The modulation times determine the duration of perturbations in a liquid and are especially sensitive to changes in interactions between probe particles and their surroundings.

If modulation processes are fast (flexible environment; weak, nonspecific interactions), $\tau_\omega \rightarrow 0$ and can be treated as times between collisions, τ_{BC}. In this case, the Enskog model[46] can be used for quick estimates of τ_{BC}:

$$\tau_{BC} = \frac{1}{4\sigma^2 N}\left(\frac{2\mu}{\pi kT}\right)^{1/2} \quad (7)$$

where σ is the collision diameter, N is the number density of particles, μ is the reduced mass of colliding particles, k is the Boltzmann constant, and T is the temperature. In the slow modulation limit (rigid quasi-lattice; strong, specific, directed interactions), $\tau_\omega \rightarrow \infty$. The second moment (perturbation dispersion) increases if collisions are fast and strong and deeply perturb interparticle potential penetrating its repulsion branch or if repulsion forces prevail, especially upon rising pressure, while a decrease in $M(2)$ signifies the dominance of attraction forces as a result of (temporary) bonding.[47,48]

Performing Fourier transforms of the time-correlation function, eq 5, in the fast and slow modulation limits, one gets Lorentzian and Gaussian limiting line profiles, respectively.

Spectroscopic Data: Dynamics. Computations have been performed according to the method described in refs 35 to 37. Representative time-correlation functions of vibrational dephasing are shown in Figures 5 to 7. The values of dephasing and modulation times are collected in Table 1.

An analysis of the dynamics of the dimethyl sulfone molecules supports the statement regarding the solvation of Li^+ in perchlorate solutions and the absence of solvation of Li^+ in nitrate solutions, as made in line shift studies. Time-correlation functions of vibrational dephasing of the $\nu_5(A_1)$ vibration of the SO_2 group of $(CH_3)_2SO_2$ in the neat dimethyl sulfone and its mixture with $LiClO_4$ are considerably different (Figure 6). In the solution, vibrational dephasing becomes faster, the values of second moments increase, and modulation times decrease (Table 1). This trend perfectly coincides with that found by Perelygin and Krauze for several vibrations of pyridine and acetone molecules involved in solvation processes in ionic solutions.[49,50] An increase in $M(2)$ upon solvation reflects stronger collisions between Li^+ and $(CH_3)_2SO_2$ than between solvent molecules, whereas τ_ω decreases due to the enrichment of the surroundings of the heavy and slow dimethyl sulfone molecules with the light, mobile lithium ions. In other words, from the point of view of vibrational dynamics, dimethyl sulfone molecules clearly tend to surround lithium ions but do not form long lasting aggregates (chemical bonds) with them.

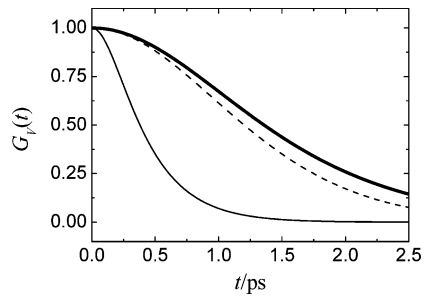

Figure 6. Time-correlation functions of the $\nu_5(A_1)$ vibration of the $(CH_3)_2SO_2$ molecule in the neat liquid. Thick solid line, neat liquid at 180 °C; thin solid line, $LiClO_4 + (CH_3)_2SO_2$ at 200 °C; dashed line, $LiNO_3 + (CH_3)_2SO_2$ at 180 °C.

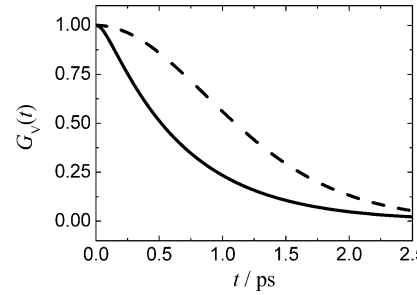

Figure 7. Time-correlation functions of the $\nu_1(A_1)$ vibration of ClO_4^- ion in the $LiClO_4 + (CH_3)_2SO_2$ system at 200 °C. Solid line, free anion; dashed line, ion pair.

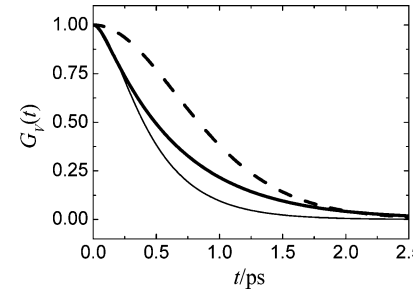

Figure 8. Time-correlation functions of the $\nu_1(A'_1)$ vibration of NO_3^- ion in the $LiNO_3 + (CH_3)_2SO_2$ system at 180 °C and in molten $LiNO_3$ at 255 °C. Thick solid line, free anion; dashed line, ion pair; thin solid line, molten salt.

On the contrary, changes in time-correlation functions of the $\nu_5(A_1)$ vibration upon adding lithium nitrate to dimethyl sulfone are insignificant (Figure 6). Both in the neat liquid and in the solution, τ_V, $M(2)$, and τ_ω remain almost the same (Table 1), thus signifying that the solvent does not form solvates with the lithium ion and its structure remains similar to that in the single liquid or that these solvates are unstable. Therefore, we suggest that the dimethyl sulfone molecules in $LiNO_3$ solutions are not involved in any interactions with Li^+ and stay away from cations.

Time-correlation functions of vibrational dephasing for free ions and ion pairs in the $LiClO_4 + (CH_3)_2SO_2$ system are significantly different in shape (Figure 7). This is due to differences in modulation processes causing vibrational dephasing of these entities. As follows from Table 1, in spite of comparable values of dephasing times, the totally symmetric $\nu_1(A_1)$ vibration of the free ion represented by the low-frequency line is modulated by a fast process (small τ_ω), and its time-correlation function has a great $M(2)$, whereas the vibration of the ion paired anion represented by the high-frequency line is modulated by a slow process (great τ_ω) due to directed $Li^+ - ClO_4^-$ interactions, and its time-correlation function has a small $M(2)$ reflecting attraction between the cations and the anions.

The shape of time-correlation functions of vibrational dephasing for two types of nitrate ions present in the $LiNO_3 + (CH_3)_2SO_2$ system is also different (Figure 8). It appears, however, that, unlike the $LiClO_4 + (CH_3)_2SO_2$ system, the vibration represented by the low-frequency line is modulated by a slow process (great τ_ω), and its time-correlation function has a small $M(2)$ reflecting attraction between the cations and the anions, whereas the vibration represented by the high-frequency line is modulated by a fast process (small τ_ω), and its time-correlation function has a great $M(2)$ (Table 1). In other

words, the high-frequency line seems to belong to the free ion and the low-frequency line to an ion pair.

Furthermore, the peak frequency, $M(2)$, and τ_ω values for high-frequency vibration are close to those for NO_3^- in molten salts[51,52] where no association between cations and anions has been observed.[53] On the other hand, the peak frequency of the low-frequency line appears quite close to that of the contact ion pair Li^+ NO_3^- isolated in an argon matrix.[54,55] Therefore, it is tempting to suggest that, in the $LiNO_3 + (CH_3)_2SO_2$ system, unlike other systems studied to date,[13] the totally symmetric $\nu_1(A'_1)$ vibrations of the free NO_3^- are represented by the high-frequency lines, and the low-frequency lines correspond to vibrations of NO_3^- in the ion pairs. If this assumption is true, one may claim that, in the $LiNO_3 + (CH_3)_2SO_2$ system, both components do not significantly interact and prefer to keep the molecular structure characteristic to the neat liquids. The dissociation of lithium nitrate in dimethyl sulfone is low, and in the regions reach in $LiNO_3$, nitrate ions are as free as in the melt, whereas in the regions reach in $(CH_3)_2SO_2$, dimethyl sulfone molecules are as free as in the neat liquid. Since the temperature is low, the tendency of Li^+ and NO_3^- to form an ion pair is pronounced, and the contact ion pairs Li^+ NO_3^- are another component of the solution. These statements agree well with the phase diagram, calculations of the liquidus curves, and conductivity measurements.

Conclusions

Studies of phase diagrams and conductivity isotherms reveal that the $LiClO_4 + (CH_3)_2SO_2$ system behaves like typical electrolytic systems containing a lithium salt and a solvent. The formation of a 1:1 solvate is clearly seen in this system, and its conductivity isotherm demonstrates a maximum. Unlike typical electrolytic systems with lithium salts, the phase diagrams of the $LiNO_3 + (CH_3)_2SO_2$ and $LiNO_3 + (C_2H_5)_2SO_2$ systems appear to be simple eutectic. The dependences of specific conductivity on the concentration of $LiNO_3$ are also uncommon, showing no maximum characteristic to electrolyte solutions. Raman studies and an analysis of dynamics performed using Raman data signify that, in the $LiClO_4 + (CH_3)_2SO_2$ system, solvated cations and contact ion pairs exist. In the $LiNO_3 + (CH_3)_2SO_2$ system, contact ion pairs are present as well, but signatures of cation solvation cannot be found.

In spite of the fact that spectroscopic studies of dynamics have been widely performed with molecular, ionic liquids and aqueous solutions,[12,36,37,42,43,53] their applications to solutions of inorganic salts in dipolar aprotic solvents are quite rare.[41,49,50] As follows from this paper, information regarding vibrational dynamics appears helpful in interpreting solvation phenomena. Small line shifts accompanying solvation in the case of dimethyl sulfone make conclusions regarding solvation tentative. An analysis of time-correlation functions enables one to prove that, in the nitrate solutions, Li^+ does not perturb the solvent molecules and their vibrational dynamics remains as the same as in the neat liquid, whereas in the perchlorate solutions, dimethyl sulfone molecules definitely tend to surround lithium cations. Moreover, this analysis is crucial for a correct assignment of vibrational lines to free ions and ion pairs in the $LiNO_3 + (CH_3)_2SO_2$ system.

It should be also noticed that spectroscopic anomalies are quite characteristic to nitrates and distinguish them from systems containing tetrahedral ions like perchlorate.[56] One may speculate that these are due to its planar geometry which, unlike the quasi-spherical shape of perchlorate, leads to significant asymmetry in properties.

Interestingly, in spirit of the dynamic criteria of complex formation,[57−59] the lower limit of lifetime of solvates in the $LiClO_4 + (CH_3)_2SO_2$ system should be considered equal to the dephasing time (0.46 ps), whereas the modulation time determines the lower limit of lifetime of the contact ion pairs: 3.51 ps in the $LiClO_4 + (CH_3)_2SO_2$ system and 2.33 ps in the $LiNO_3 + (CH_3)_2SO_2$ system. These values agree well with existing estimates.[10,11,14]

It has been concluded in a recent analysis[15] that, in the measurement of ion pairing, conventional spectroscopic methods often fail. We guess that the extension of dynamical approaches to the studies of solvation and ion pairing phenomena, like that performed in refs 49 and 50 and this work, is undoubtedly fruitful and enables one to decrease the ambiguity of conclusions based on spectroscopic data alone. In particular, the trends in changing time-correlation functions of vibrational dephasing accompanying the solvation and formation of contact ion pairs are evident. For solvent molecules, a decrease in modulation times and increase in the vibrational second moments, as found by Perelygin and Krauze[49,50] and supported in this paper, is characteristic to solvation processes. Spectroscopically, in accordance with eq 5 and its Fourier transform, this means that, upon solvation, the lines of the solvent molecules corresponding to the vibrations of the functional groups coordinated to cations become more Lorentzian in shape than in free solvents. For anions, an increase in modulation times and decrease in the vibrational second moments, as established in this paper, is peculiar to the formation of contact ion pairs. Spectroscopically, this means that the lines of ion paired anions become more Gaussian in shape than those of free anions. A trend in changing time-correlation functions of vibrational dephasing accompanying the formation of solvent-separated ion pairs[41] is less definite and should be clarified to obtain a complete picture of the influence of solvation and ion pairing processes on vibrational line shapes and dynamics of anions and solvent molecules in ionic solutions.

Supporting Information Available:

Thermal analysis data, representative thermal analysis curves, and conductivity data measured in this work. This material is available free of charge via the Internet at http://pubs.acs.org.

Literature Cited

(1) Gores, H. J.; Barthel, J. M. G. Nonaqueous Electrolyte Solutions: New Materials for Devices and Processes Based on Recent Applied Research. *Pure Appl. Chem.* **1995**, *67*, 919–930.
(2) Xu, K. Nonaqueous Liquid Electrolytes for Lithium-Based Rechargeable Batteries. *Chem. Rev.* **2004**, *104*, 4303–4418.
(3) Janz, G. J.; Tomkins, R. P. T. *Nonaqueous Electrolytes Handbook*, Vol. 1; Academic Press: New York, 1972.
(4) Janz, G. J.; Tomkins, R. P. T. *Nonaqueous Electrolytes Handbook*, Vol. 2; Academic Press: New York, 1973.
(5) Barthel, J. Transport Properties of Electrolytes from Infinite Dilution to Saturation. *Pure Appl. Chem.* **1985**, *57*, 355–367.
(6) Bockris, J. O'M.; Reddy, A. K. N. *Modern Electrochemistry*, Vol. 1, 2nd ed.; Plenum: New York, 1998.
(7) Ohtaki, H.; Radnai, T. Structure and Dynamics of Hydrated Ions. *Chem. Rev.* **1993**, *93*, 1157–1204.
(8) Neilson, G. W.; Adya, A. K. Neutron Diffraction Studies of Liquids. *Annu. Rep. Chem. C* **1997**, *93*, 101–145.
(9) Rode, B. M.; Schwenk, C. F.; Tongraar, A. Structure and Dynamics of Hydrated Ions - New Insights through Quantum Mechanical Simulations. *J. Mol. Liq.* **2004**, *110*, 105–122.
(10) Rode, B. M.; Schwenk, C. F.; Hofer, T. S.; Randolf, B. R. Coordination and Ligand Exchange Dynamics of Solvated Metal Ions. *Coord. Chem. Rev.* **2005**, *249*, 2993–3006.
(11) Marcus, Y.; Hefter, G. Ion Pairing. *Chem. Rev.* **2006**, *106*, 4585–4621.
(12) James, D. W. Spectroscopic Studies of Ion-Ion-Solvent Interactions in Solutions Containing Oxyanions. *Prog. Inorg. Chem.* **1985**, *33*, 353.

(13) Perelygin, I. S. Infra-Red Spectra and Solvation of Ions. In *Ionic Solvation*; Krestov, G. A., Ed.; Ellis Horwood: Chichester, 1994; p 100−207.
(14) Barthel, J. Ion Solvation and Ion Association Studied by Infrared and Microwave Methods. *J. Mol. Liq.* **1995**, *65*−*66*, 177–185.
(15) Hefter, G. When Spectroscopy Fails: The Measurement of Ion Pairing. *Pure Appl. Chem.* **2006**, *78*, 1571–1586.
(16) Klassen, B.; Aroca, R.; Nazri, M.; Nazri, G. A. Raman Spectra and Transport Properties of Lithium Perchlorate in Ethylene Carbonate Based Binary Solvent Systems for Lithium Batteries. *J. Phys. Chem. B* **1998**, *102*, 4795–4801.
(17) Brouillette, D.; Irish, D. E.; Taylor, N. J.; Perron, G.; Odziemkowski, M.; Desnoyers, J. E. Stable Solvates in Solution of Lithium Bis(trifluoromethylsulfone)imide in Glymes and Other Aprotic Solvents: Phase Diagrams, Crystallography and Raman Spectroscopy. *Phys. Chem. Chem. Phys.* **2002**, *4*, 6063–6071.
(18) Alía, J. M.; Edwards, H. G. M.; Lawson, E. E. Preferential Solvation and Ionic Association in Lithium and Silver Trifluomethanesulfonate Solutions in Acrylonitrile/Dimethylsulfoxide Mixed Solvent: A Raman Spectroscopic Study. *Vib. Spectrosc.* **2004**, *34*, 187–197.
(19) Burba, C. M.; Frech, R. Spectroscopic Measurements of Ionic Association in Solutions of $LiPF_6$. *J. Phys. Chem. B* **2005**, *109*, 15161–15164.
(20) Alves, W. A. Vibrational Spectroscopic Characterization of Stable Solvates in the $LiClO_4$/Formamide:Acetonitrile System. *J. Mol. Struct.* **2007**, *829*, 37–43.
(21) Alves, W. A. Vibrational Spectroscopic and Conductimetric Studies of Lithium Battery Electrolyte Solutions. *Vib. Spectrosc.* **2007**, *44*, 197–200.
(22) Xu, K.; Angell, C. A. High Anodic Stability of a New Electrolyte Solvent: Unsymmetric Noncyclic Aliphatic Sulfone. *J. Electrochem. Soc.* **1998**, *145*, L70–L72.
(23) Clark, T.; Murray, J. S.; Lane, P.; Politzer, P. Why Are Dimethyl Sulfoxide and Dimethyl Sulfone Such Good Solvents. *J. Mol. Model.* **2008**, *14*, 689–697.
(24) Legrand, L.; Heintz, M.; Tranchant, A.; Messina, R. Sulfone-Based Electrolytes for Aluminum Electrodeposition. *Electrochim. Acta* **1994**, *40*, 1711–1716.
(25) Shu, M.-F.; Hsu, H.-Y.; Yang, C.-C. Physical Properties of a New Type of Molten Electrolytes, $ZnCl_2$-$DMSO_2$. *Z. Naturforsch.* **2003**, *58a*, 451–456.
(26) Biagini, P.; Calderazzo, F.; Marchetti, F.; Pampaloni, G.; Ramello, S.; Salvalaggio, M.; Santi, R.; Spera, S. Mono- and Dinuclear Complexes of Sulfones with the Tetrachlorides of Group 4. *Dalton Trans.* **2004**, 2364–2371.
(27) Tretyakov, D. O.; Prisiazhnyi, V. D. Physico-Chemical Properties of $LiBF_4$ - Dimethyl Sulfone and Diethyl Sulfone Melts. *Ukr. Khem. Zh.* **2004**, *70*, 37–38.
(28) Potapenko, A. V.; Kramarenko, A. A.; Prisiazhnyi, V. D. Cathode Reduction of Sulfur in a $LiN(CF_3SO_2)_2$ - Diglyme Salt-Solvate Electrolyte. *Ukr. Khem. Zh.* **2002**, *68*, 57–60.
(29) Fateev, S. A.; Nizhnikovkii, E. A. High-Temperature Lithium - Fluorocarbon Battery. *Electrochem. Energy Systems* **2005**, *5*, 106–108.
(30) Henderson, W. A. Glyme-Lithium Salt Phase Behavior. *J. Phys. Chem. B* **2006**, *110*, 13177–13183.
(31) Daniels, F.; Alberty, R. A. *Physical Chemistry*; Wiley: New York, 1955; Chapter 8.
(32) Xu, Q.; Ma, Y.; Qui, Z. Calculation of Thermodynamic Properties of LiF-AlF_3, NaF-AlF_3 and KF-AlF_3. *CALPHAD: Comput. Coupling Phase Diagrams Thermochem.* **2001**, *25*, 31–42.
(33) Database on Thermal Constants of Substances; United Institute for High Temperatures, Russian Academy of Sciences, and Department of Chemistry, Moscow State University. http://www.chem.msu.ru/cgi-bin/tkv.pl?show=welcome.html (accessed Dec 17, 2009).
(34) Zhang, S. S.; Angell, C. A. A Novel Electrolyte Solvent for Rechargeable Lithium and Lithium-Ion Batteries. *J. Electrochem. Soc.* **1996**, *143*, 4047–4053.
(35) Kirillov, S. A. Time-Correlation Functions from Band-Shape Fits without Fourier Transform. *Chem. Phys. Lett.* **1999**, *303*, 37–42.
(36) Kirillov, S. A. Spectroscopy of Interparticle Interactions in Ionic and Molecular Liquids: Novel Approaches. *Pure Appl. Chem.* **2004**, *76*, 171–182.
(37) Kirillov, S. A. Novel Approaches in Spectroscopy of Interparticle Interactions. Vibrational Line Profiles and Anomalous Non-Coincidence Effects. In *Novel approaches to the structure and dynamics of liquids: Experiments, theories and simulations*, NATO ASI Series; Samios, J., Durov, V., Eds.; Kluwer: Dordrecht, 2004; pp 193−227.
(38) Siebert, H. *Anwendungen in der Schwingungsspectroscopie in der anorganischen Chemie*; Springer: Berlin, 1966.
(39) McLachlan, R. D.; Carter, V. B. Vibrational Spectra of Crystalline Dimethyl Sulfone. *Spectrochim. Acta* **1970**, *26A*, 1121–1127.
(40) Legrand, L.; Tranchant, A.; Messina, R.; Romain, F.; Lautie, A. Raman Study of Aluminum Chloride-Dimethylsulfone Solutions. *Inorg. Chem.* **1996**, *35*, 1310–1312.
(41) Perelygin, I. S.; Mikhaylov, G. P. Vibrational and Orientational Relaxation of Nitrate Ion in a Dipolar Aprotic Solvent. *Chem. Phys. (Russ. Ed.)* **1988**, *7*, 880–884.
(42) Rothschild, W. G. *Dynamics of Molecular Liquids*; Wiley: New York, 1984.
(43) Wang, C. H. *Spectroscopy of Condensed Media. Dynamics of Molecular Interactions*; Academic: Orlando, FL, 1985.
(44) Oxtoby, D. W. Dephasing of Molecular Vibrations in Liquids. *Adv. Chem. Phys.* **1979**, *40*, 1–48.
(45) Kubo, R. A. Stochastic Theory of Line-Shape and Relaxation. In *Fluctuations, Relaxation and Resonance in Magnetic Systems*, Scottish Universities' Summer School 1961; ter Haar, G., Ed.; Oliver and Boyd: Edinburgh, 1962; pp 23−68.
(46) Dardi, P. S.; Cukier, R. I. Vibrational relaxation in fluids: A critical analysis of the independent binary collision theory. *J. Chem. Phys.* **1988**, *89*, 4145–4153.
(47) Schroeder, J.; Schiemann, V. H.; Sharko, P. T.; Jonas, J. Raman Study of Vibrational Dephasing in Liquid CH_3CN and CD_3CN. *J. Chem. Phys.* **1977**, *66*, 3215–3226.
(48) Schindler, W.; Sharko, P. T.; Jonas, J. Raman Study of Pressure Effects on Frequencies and Isotropic Line Shapes in Liquid Acetone. *J. Chem. Phys.* **1982**, *76*, 3493–3496.
(49) Perelygin, I. S.; Krauze, A. S. Raman Spectra and Dynamics of Pyridine Molecules in Ionic Solutions. *Chem. Phys. (Russ. Ed.)* **1988**, *7*, 1231–1239.
(50) Perelygin, I. S.; Krauze, A. S. Vibrational and Orientational Relaxation of Acetone Molecules in Ionic Solutions. *Chem. Phys. (Russ. Ed.)* **1989**, *8*, 1043–1049.
(51) Kato, T.; Takenaka, T. Raman Study of Rotational Motion and Vibrational Dephasing Dynamics of NO_3^- in Molten Nitrates. *Mol. Phys.* **1985**, *54*, 1393–1414.
(52) Kirillov, S. A.; Gorodyskii, A. V. Ionic Dynamics of Molten Lithium Nitrate in Picosecond Time Domain. *Dokl. Akad. Nauk SSSR* **1986**, *287*, 162–164.
(53) Kirillov, S. A. Interactions and Picosecond Dynamics in Molten Salts: A Review with Comparison to Molecular Liquids. *J. Mol. Liq.* **1998**, *76*, 35–95.
(54) Smith, D.; James, D. W.; Devlin, J. P. Vibrational Spectra of Molecular Metal Nitrate Monomers and Dimers. *J. Chem. Phys.* **1971**, *54*, 4437–4442.
(55) Moore, J. C.; Devlin, J. P. Ion Pair and Partially Hydrated Li^+ NO_3^- Ion Pair Structures: Correlation of Molecular Orbital Results with Matrix Isolation Data. *J. Chem. Phys.* **1978**, *68*, 826–831.
(56) Gafurov, M. M.; Aliev, A. R. Molecular Relaxation Processes in the Salt Systems Containing Anions of Various Configurations. *Spectrochim. Acta* **2004**, *60A*, 1549–1555.
(57) Wilmshurst, J. K. Infrared Spectra of Highly Associated Liquids and the Question of Complex Ions in Fused Salts. *J. Chem. Phys.* **1963**, *39*, 1779–1788.
(58) Kirillov, S. A.; Pavlatou, E. A.; Papatheodorou, G. N. Instantaneous Collision Complexes in Molten Alkali Halides: Picosecond Dynamics from Low-Frequency Raman Data. *J. Chem. Phys.* **2002**, *116*, 9341–9351.
(59) Kirillov, S. A. Vibrational Spectra of Fused Salts and Dynamic Criterion of Complex Formation in Ionic Liquids. *J. Mol. Struct.* **2003**, *651*−*653*, 289–293.

Received for review October 30, 2009. Accepted February 2, 2010. This work has been carried out within the framework of Ukrainian-Russian bilateral collaboration with partial financial support from Ukrainian National Academy of Sciences and Russian Foundation for Basic Research.

JE9009249